Synthesis and characterization of a hydrophilic conjugated 4+4 Re(I)-porphyrin metallacycle

Domenico Milano, Luka Đorđević, Ennio Zangrando, Elisabetta Iengo* and Paolo Tecilla*

Department of Chemical and Pharmaceutical Sciences, University of Trieste, via Giorgieri 1, I-34127, Trieste, Italy. E-mail: eiengo@units.it, ptecilla@units.it

Abstract: The preparation and the full characterization, including the X-ray structure determination, of a polar *trans*-dipyridylporphyrin functionalized with two short polyoxyethylene chains is reported. Reaction of the porphyrin with a Re(I) complex yielded a 4+4 metallacycle showing an improved solubility and a lower tendency to aggregate with respect to analogous porphyrin cyclic derivatives. These properties allowed a full NMR characterization of the metallacycle including VT ^{1}H DOSY-NMR experiments and, for the first time, the recording of a ^{13}C-NMR spectrum giving further insight into the structural definition of these type of metallacycles. Spray deposition of the metallacycle on a heated mica substrate shows the formation of regular ring-like nano-structures which are not formed by the parent porphyrin.

Keywords: metal mediated self-assembling, *trans*-di(4-pyridyl)porphyrin, Re(I), metallacycle,

1. Introduction

The self-assembly of supramolecular ensembles based on organic polytopic ligands and metal centers has attracted increasing attention in the last years. Indeed, following this "bottom-up" approach, complex functional architectures become readily accessible simply by synthesizing easy to make building blocks and letting them self-organize. In this context, over the years, the metal-mediated directional-bonding approach has proved to be an effective methodology to build complex 2D and 3D supramolecular architectures [1]. One of the most appealing features of this approach is the possibility to predict, to some extent, structure and thermodynamic and kinetic stability of the final ensembles simply reasoning on the geometrical and chemical characteristics of the rigid polytopic organic ligands and of the complementary metal fragments [2]. This has led to the collection of a variety of chemical bonding tools that constitutes a rich molecular tool-box from which the supramolecular chemist may pick the proper elements to construct the designed final supramolecular structure. Among the many organic ligands contained in this tool-box, porphyrin-

based ligands and, in particular, *meso* substituted pyridylporphyrins, play a prominent role due to their peculiar geometrical and electronic properties [3] In fact, conjugation of these chromophoric ligands with different metal ions ((Pd(II), Pt(II), Ru(II), Re(I)) has led to the development of a variety of coordination adducts with interesting potential applications in the fields of optoelectronics, catalysis, molecular recognition, etc. [4].

A particularly interesting class of discrete systems are porphyrin metallacycles formed by combination of *trans*-dipyridylporphyrin ligands with the *cis*-coordinating *fac*-Re(I)$(CO)_3X$ (X = Br^- or Cl^-) fragment, which ensures high thermodynamic and kinetic stability to the derived supramolecular adducts at room temperature. Work pioneered by the group of J. T. Hupp has shown that, in weakly coordinating solvents, such as a mixture of toluene and tetrahydrofuran, the 1:1 combination of $Re(CO)_5X$ and a *trans*-dipyridylporphyrin ligand generally produces 4+4 neutral metallacycles, of general formula [Re(I)$(CO)_3$X(*trans*-dipyridylporphyrin)]$_4$, in high yield [5]. These supramolecular adducts have a roughly cubical box structure with edges about 2 nm long and display an exceptional stability, even in competing media. As a matter of fact, we have shown that one such 4+4 Re(I)-porphyrin metallacycle is stable in a phospholipid bilayer, in which it forms dimeric nanopores [6] while the use of alternative metal fragments, based on for example Pd(II), gives kinetically labile adducts, resulting in complex mixtures of linear oligomers and cyclic adducts [7].

Despite their interesting properties, the number of such adducts described in the literature is still limited and this is probably a consequence of the non-trivial synthesis of the porphyrin precursors, of the scarce solubility and difficult characterization of their Re(I) adducts. As a matter of fact, up to day, there are not available X-ray structures of these metallacycles and the only direct evidences of their structures and nuclearities are based on one FAB mass spectrum [8], on the determination of the molecular weight by vapor-phase osmometry [9], on the estimation of the molecular size by gel permeation chromatography [10], and by pulsed-field-gradient NMR [11]. Moreover, the low solubility in all the common solvents, combined with possible different conformations as a consequence of the rotation around the Re-pyridyl bond [12], makes the NMR analysis of these neutral metallacyclic adducts quite complex. With the aim to address the solubility issue, we have recently reported two new 4+4 Re(I)-porphyrin metallacycles in which the phenyl substituent on the free *meso* position of the porphyrins were functionalized with alkyl chains of different lengths [13]. However, contrary to our expectations, this type of substitution resulted in an even poorer solubility of the derived adducts. We therefore decided to explore the possibility of introducing more hydrophilic substitutions, and here we report the results obtained using a *trans*-dipyridylporphyrin bearing two short polyoxyethylene chains. In particular, the resulting 4+4 Re(I)-

porphyrin metallacycle shows a good solubility in common organic solvents allowing, for the first time, a full NMR characterization, including ^{13}C-NMR spectra and VT-^{1}H-DOSY experiments.

2. Experimental

2.1 General methods

All commercially available reagents were purchased from Sigma-Aldrich, Fluka and Strem Chemicals and used without purification unless otherwise mentioned. Solvents were purchased from Aldrich, VWR, Fluka and Riedel, and deuterated solvents from Cambridge Isotope Laboratories and Aldrich. Analytical thin layer chromatography (TLC) was carried out on Merck silica gel plates (thickness 0.25 mm). Column chromatography (CC) was carried out on Merck silica gel 60 (40–63 and 230–400 mesh).

NMR spectra were recorded on a Varian 500 MHz spectrometer (operating at 500 MHz for ^{1}H and at 125 MHz for ^{13}C). Chemical shifts are reported as parts per million (ppm) relative to the solvent residual signal as internal reference. IR spectra were recorded on a Perkin Elmer 2000 NIR spectrophotometer with the KI or KBr pellet technique. UV-Vis spectra were recorded on a Perkin Elmer Lambda 35 spectrophotometer. Fluorescence emission spectra were recorded on a Varian Cary Eclypse spectrofluorimeter. Electrospray ionization mass spectra (ESI-MS) were performed on a Perkin Elmer APII at 5600 eV.

AFM measurements were carried out in air at room temperature by using a Nanoscope IIIa (Digital Instruments Metrology Group, USA) instrument, model MMAFMLN. The collected images were then analyzed with WsXm 4.0 software (Nanotec Electronica S. L.), and Gwyddion 2.42.

5-(4-Pyridyl)dipyrromethane (DPM-Py) [14], 4-{2-[2-(2-methoxyethoxy)ethoxy]ethoxy} benzaldehyde (TegPhCHO) [15], and [$ReBr(CO)_5$] [16] were prepared following literature procedures.

Abbreviations used in the text: DCM = dichloromethane; THF = tetrahydrofuran; DMSO = dimethylsulfoxide; TFA = trifluoroacetic acid; DDQ = 2,3-dichloro-5,6-dicyano-1,4-benzoquinone; TLC = thin layer chromatography.

2.2 Synthesis of 5,15-Bis-(4-pyridyl)-10,20-bis-(4-[2-[2-(2-methoxyethoxy)ethoxy]ethoxy] phenyl) porphyrin (DiTegPhDPyP).

The reaction was conducted under Ar atmosphere and in the dark. TegPhCHO (329 mg, MW = 268.31, 1.22 mmol) was dissolved in anhydrous DCM (150 mL) and the solution was cooled, with an ice bath, to 0 °C. TFA (6.0 mL, MW = 114.02, d = 1.535 g/mL, 81.0 mmol) was then added

dropwise. Finally, DPM-Py (273 mg, MW = 223.27, 1.22 mmol) was added and the reaction mixture was stirred for 1 hour. The reaction mixture was left to reach room temperature and with no more inert atmosphere, DDQ (1.18 g, MW = 227.0, 5.2 mmol) was added and the mixture was kept under stirring for 2 hours. The reaction mixture was directly washed with saturated $NaHCO_{3\,(aq)}$ and water, the organic phase was dried over anhydrous Na_2SO_4 and the solvent removed under vacuum. Purification by column chromatography (silica gel, $CHCl_3$/MeOH 99:1 *v/v*) and crystallization from $CHCl_3$/MeOH afforded 111 mg of a dark purple solid. Yield 20%. R_f = 0.46 (SiO_2, $CHCl_3$/MeOH 95/5 *v/v*). ^{1}H-NMR (500 MHz, $CDCl_3$), δ_H, ppm: 9.04 (4H, dd, *J* = 6.0, 1.5 Hz, H-2,6 Py), 8.92 (4H, d, *J* = 4.5 Hz, H-β Pyrr), 8.80 (4H, d, *J* = 5.0 Hz, H-β Pyrr), 8.17 (4H, dd, *J* = 6.0, 2.0 Hz, H-3,5 Py), 8.1 (4H, d, *J* = 8.5 Hz, H-2,6 Ph), 7.32 (4H, d, *J* = 8.5 Hz, H-3,5 Ph), 4.44 (4H, m, PhOC*H*$_2$CH$_2$O), 4.07 (4H, m, OCH$_2$C*H*$_2$O), 3.89 (4H, m, OC*H*$_2$CH$_2$O), 3.80 (4H, m, OCH$_2$C*H*$_2$O), 3.75 (4H, m, OC*H*$_2$CH$_2$O), 3.62 (4H, m, OCH$_2$C*H*$_2$OCH$_3$), 3.42 (6H, s, OCH$_3$), –2.83 (2H, br, NH). ^{13}C-NMR (125 MHz, $CDCl_3$), δ_C, ppm: 159.0, 150.4, 148.4, 135.7, 134.3, 129.5, 126.6, 122.4, 120.8, 120.3, 117.0, 113.1, 111.7, 72.1, 71.1, 70.9, 70.8, 70.0, 67.9, 59.2. ESI-MS (m/z): for $C_{56}H_{56}N_6O_8$ calculated 940.416; found 941.6 $[M+H]^+$, 963.5 $[M+Na]^+$. UV-Vis (CH_2Cl_2), λ_{max} (nm) (relative intensity, %): 419 (100), 516 (5.2), 550 (3.0), 592 (1.9), 651 (2.7). Fluorescence Emission (**(**CH_2Cl_2, λ_{exc} 426 nm), λ_{em} (nm): 655, 719. IR (KBr), ν (cm^{-1}): 3078, 2922, 2860, 1637, 1593, 1449, 1404, 1384, 1351, 1286, 1246, 1175, 1108, 967, 788, 737.

2.3 Synthesis of [Re(CO)$_3$(DiTegPhDPyP)Br]$_4$.

DiTegPhDPyP (50 mg, MW = 941.08, 0.053 mmol) and $Re(CO)_5Br$ (21.6 mg, MW = 406.13, 0.053 mmol) were dissolved in a mixture of anhydrous toluene-THF (45 mL, 4:1 *v/v*), under Ar atmosphere. The reaction mixture was heated to reflux and kept under stirring. After 24 hours, when the starting porphyrin disappeared and no more changes were observed on TLC, the heating was stopped and the solvent removed under vacuum. Purification by column chromatography (silica gel, $CHCl_3$/MeOH from 99:1 to 98:2 *v/v*) afforded 19.7 mg of a light purple solid. Yield 33%. R_f 0.8 (SiO_2, $CHCl_3$/MeOH 95:5 *v/v*). ^{1}H-NMR (500 MHz, $CDCl_3$), δ_H, ppm: 9.50 (d, *J* = 6.5 Hz 16H, H-2,6 Py), 8.89 (d, *J* = 5.0 Hz, 16H, H-β Pyrr), 8.83 (d, *J* = 4.5 Hz, 16H, H-β Pyrr), 8.34 (d, *J* = 6.5 Hz, 16H, H-3,5 Py), 7.97 (d, *J* = 8.5 Hz, 16H, H-2,6 Ph), 7.15 (d, *J* = 9 Hz, 16H, H-3,5 Ph), 4.23 (m, 8H, PhO*CH*$_2$CH$_2$O), 3.85 (m, 8H, OCH$_2$*CH*$_2$O), 3.66 (m, 8H, O*CH*$_2$CH$_2$O), 3.54 (m, 8H, OCH$_2$*CH*$_2$O), 3.46 (m, 8H, O*CH*$_2$CH$_2$O), 3.35 (m, 8H, OCH$_2$*CH*$_2$OCH$_3$), 3.22 (s, 24H, OCH$_3$), −2.88 (br, 8H, NH). ^{13}C-NMR (125 MHz, $CDCl_3$, selected peaks), δ_C, ppm: 195.5, 192.7, 159.2, 153.6, 153.2, 152.5, 135.8, 133.9, 131.8, 130.3, 130.0, 129.3, 125.8, 122.0, 115.3, 113.4, 72.1, 71.1, 70.9, 70.7, 70.0, 67.9, 59.2. UV-Vis (CH_2Cl_2), λ_{max} (nm) (relative intensity, %): 426 (100), 519

(5.4), 556 (4.0), 598 (2.0), 653 (3.0). Fluorescence Emission **(**CH_2Cl_2, λ_{exc} 426 nm), λ_{em} (nm): 661, 725. IR (KI), ν (cm^{-1}): 3468, 2920, 2852, 2346, 2024, 1921, 1887, 1726, 1610, 1506, 1472, 1418, 1372, 1351, 1289, 1248, 1177, 1111, 968, 845, 802, 733.

2.4 X-ray crystallography

Data collection from a single crystal of DiTegPhDPyP was performed at the X-ray diffraction beamline (XRD1) of the Elettra Synchrotron of Trieste (Italy), with a Pilatus 2M image plate detector. The experiment was performed at 100 K (nitrogen stream supplied by an Oxford Cryostream 700) with a monochromatic wavelength of 0.700 Å through the rotating crystal method. The diffraction data were indexed, integrated and scaled using program XDS [17]. The structure was solved by direct methods using SIR2014 [18]. Fourier analysis and refinement with the full-matrix least-squares method based on F^2 were performed with SHELXL-2014 [19].

The polyoxyethylene chain was found disordered over two conformations with occupancies refined at 0.524(5)/0.476(5) with geometrical constrains applied to the bond distances. Hydrogen atoms were placed at calculated positions with isotropic U factors equal to 1.2 times the equivalent U factor of the bonded atom.

Crystal data and details of refinement: $C_{56}H_{56}N_6O_8$, M = 941.06, triclinic, space group *P*-1, a = 10.570(4), b = 10.760(9), c = 12.960(2) Å, α = 65.75(2), β= 79.01(2), γ = 61.41(2)°, V = 1180.0(11) $Å^3$, Z = 1, Dc = 1.324 g/cm^3, μ(Mo-Kα) = 0.090 mm^{-1}, F(000) = 498, θ range = 2.16 - 25.94°. Final *R*1 = 0.0767, *wR*2 = 0.1816, S = 1.113 for 372 parameters and 8623 reflections, 4418 unique [R(int) = 0.0289], of which 4269 with $I > 2\sigma(I)$, max positive and negative peaks in Δ*F* map 0.842, −0.685 e. $Å^{-3}$.

3. Results and Discussion

3.1 Synthesis of the porphyrin DiTegPhDPyP

The synthesis and the structure of the target porphyrin are shown in Scheme 1. 5,15-Bis-(4-pyridyl)-10,20-bis-(4-[2-[2-(2-methoxyethoxy)ethoxy]ethoxy]phenyl)porphyrin (DiTegPhDPyP) is an A_2B_2 *trans meso*-substituted porphyrin with two *trans meso*-positions occupied by two pyridine rings, available for metal ion coordination, and the other two by phenyl rings *para*-substituted with a triethylene glycol chain, which ensures good solubility in polar solvents. This porphyrin was previously obtained by us in low yield (3-5%) as a byproduct while preparing different A_2BC *trans meso*-substituted porphyrins [15] and its enhanced solubility properties prompted us to optimize the synthetic procedure. In particular, following the Lindsey's approach [20] the porphyrin was obtained by reacting equimolar amounts of 5-(4-pyridyl)dipyrromethane (DPM-Py), which is easily

prepared in 66% yield from 4-pyridinecarboxaldehyde and pyrrole [14], with 4-{2-[2-(2-methoxyethoxy)ethoxy]ethoxy}benzaldehyde (TegPhCHO), as shown in Scheme 1. The latter species was in turn synthesized in 60% yield, through the Mitsunobu reaction, from commercially available 4-hydroxybenzaldehyde and monomethoxytriethylene glycol [**Errore. Il segnalibro non è definito.**]. Reaction of TegPhCHO with DPM-Py under optimized conditions [13] (TFA 66 eq., DCM, 0 °C, 1h, followed by oxidation with DDQ) afforded DiTegPhDPyP in 20% yield (Scheme 1). The porphyrin was fully characterized by 1D and 2D ^{1}H-NMR, ^{13}C-NMR, ^{1}H DOSY-NMR, IR, UV-Vis, and ESI-MS spectrometry (see Supplementary Material). Crystals suitable for X-ray structural determination were grown from $CHCl_3$/MeOH and Figure 1 shows the derived molecular structure of DiTegPhDPyP. The molecule is located on a crystallographic center of symmetry with the polyoxyethylene chains disordered over two conformations, as described in the experimental section. In the crystal the porphyrins are packed in a stair-like arrangement in such a way that N4 core of each porphyrin is sandwiched by polyoxyethylene chains of symmetry related molecules (NH···H_2C proton distances of ca. 3.0 Å).

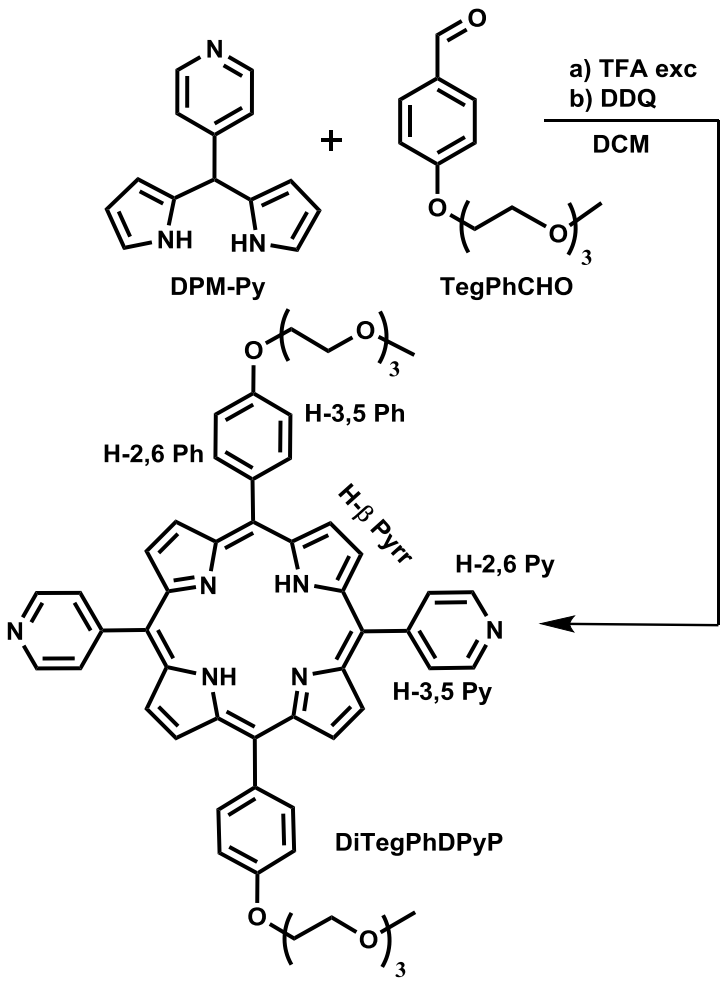

Scheme 1. Synthesis of porphyrin DiTegPhDPyP. Conditions: a) TFA 66 eq., DCM, 0 °C, 1 h, r.t., under Ar; b) DDQ 4 eq., 2 h, r.t., under air. Yield = 20%.

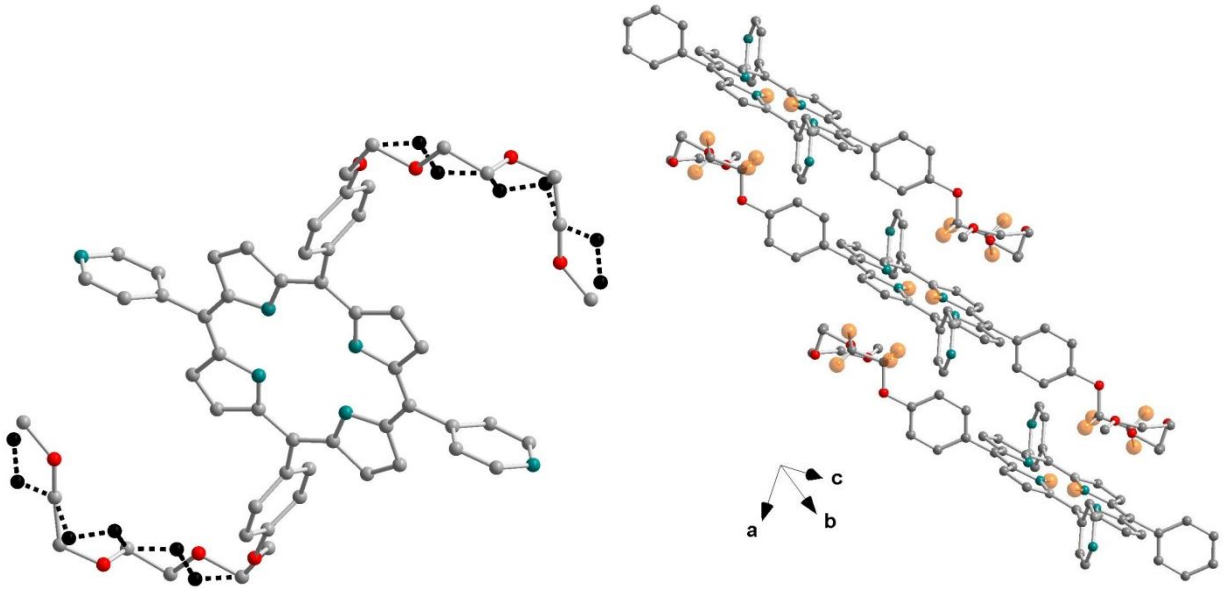

Figure 1. Molecular structure of DiTegPhDPyP (left) with indication of the disorder observed in the pendant polyoxyethylene chains (hydrogens omitted for clarity). On the right a perspective view of the crystal packing showing the porphyrin core sandwiched by methylene groups of symmetry related molecules (big yellow spheres indicate H atoms at close distance). Color code: C = grey, N = green, O = red. An Ortep view of the crystal structure is reported in Figure S14 of the Supplementary Material.

3.2 Synthesis of the $[Re(CO)_3(DiTegPhDPyP)Br]_4$ metallacycle

The group of J. T. Hupp has shown that heating equimolar amounts of $Re(CO)_5X$ (X= Cl or Br) and of a *trans meso*- dipyridylporphyrin in a mixture of toluene and tetrahydrofuran, generally produces metallacycles in high yield [5]. Indeed, while at room temperature the Re(I)–N bonds are stable, at high temperatures they are labile enough to allow for conversion of kinetic structures (such as open oligomers) to thermodynamic structures, during the assembly process. The strong *trans* labilizing effect of CO forces the replacement of only two *cis* carbonyl ligands first with solvent molecules and then with the pyridyl donors, while the *fac* geometry of the residual ones is maintained. With linear ditopic ligands, the number of Re–N bonds is maximized by forming cyclic as opposed to open oligomeric structures and the strain is minimized by forming structures having square geometry [5]. Moreover, entropy factors favors closed structures with a minimum number of components rather than polymeric structures, which involve a far larger number of components [21]. Therefore, the assembly of the 4+4 Re(I)-dipyridylporphyrin metallacycle was conducted following the procedure described by Hupp and co-workers, with some modifications [8]. Equimolar amounts of DiTegPhDPyP and $Re(CO)_5Br$ (0.053 mmol) were dissolved in 4:1 toluene-

THF (45.0 mL) and heated to reflux for 24 h (Scheme 2). After purification by column chromatography on silica, $[Re(CO)_3(DiTegPhDPyP)Br]_4$ was obtained as a purple solid in 33% yield. The metallacycle is well soluble in common solvents such as $CHCl_3$, DMSO, and THF but not in CH_3OH and H_2O and it has been characterized by ^{1}H-NMR, ^{13}C-NMR, ^{1}H DOSY-NMR, IR, and UV-Vis spectroscopies. Regrettably, and in analogy with the other reported 4+4 Re(I)-dipyridylporphyrin metallacycles, we were not able to obtain the mass spectra of the derivative despite several attempts made with different mass spectrometry techniques (ESI, MALDI, FAB).

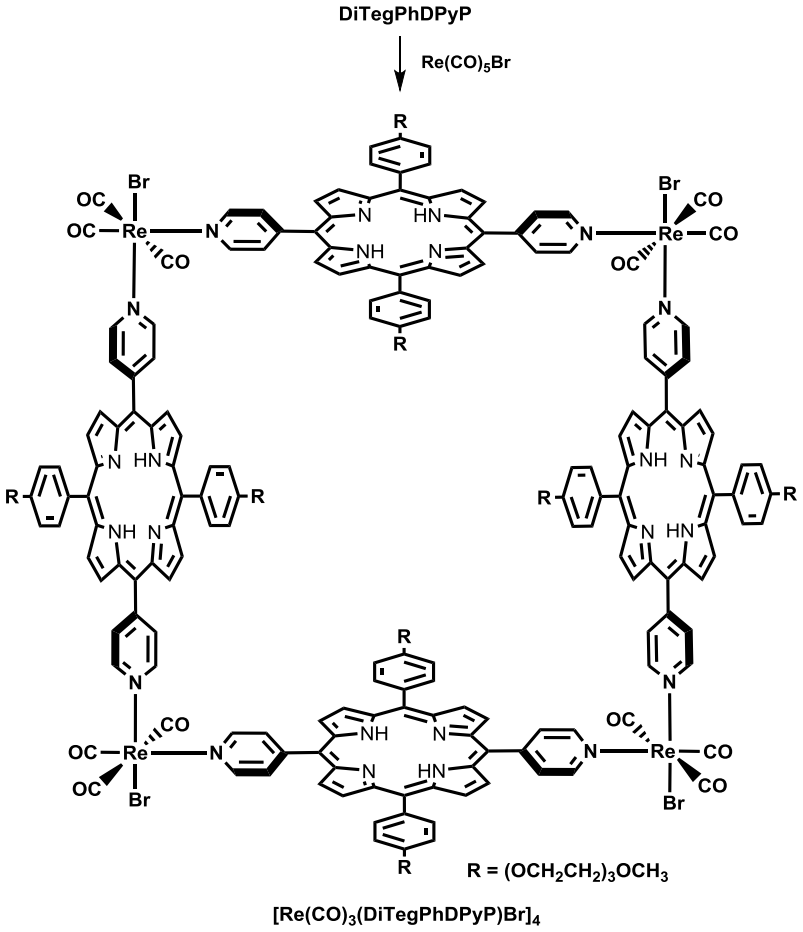

Scheme 2. Synthesis of $[Re(CO)_3(DiTegPhDPyP)Br]_4$. Conditions: toluene-THF 4:1 (*v/v*), 24 h, reflux, yield = 33%.

3.2.1 NMR characterization of the $[Re(CO)_3(DiTegPhDPyP)Br]_4$ metallacycle

As mentioned above, examples of such type of 4+4 porphyrin metallacycles reported in the literature are limited, and their full characterization remains problematic and partially unachieved. In particular, NMR solution characterization is challenging because of the inherent low solubility and high tendency to form aggregates in solution of such adducts, and may be further hampered by the rotational freedom of the porphyrin edges around the metal−pyridyl bond possibly leading to a population of conformers. In addition, further complication arises from the presumably statistical

distribution of the *syn*/*anti* isomers derived by the orientation of the halide ligand on each rhenium fragment, that can be positioned either up or down with respect to the metallacycle framework [22] As a consequence, the NMR spectra show broad and unresolved peaks, making their analysis inevitably difficult [13]. On the contrary, in $[Re(CO)_3(DiTegPhDPyP)Br]_4$ the presence of the Teg substituents has a very positive effect on the ^{1}H-NMR spectra of the metallacycle, which appears with well resolved sharp peaks (Figure 2). This is likely due to the combination of an increased solubility, a minor tendency to aggregate as a consequence of the higher polar character of the metallacycle, and to the hindered rotation of the porphyrins around the Re(I)–pyridine axis due to the large size of the Teg substituents on the *meso*-phenyl rings.

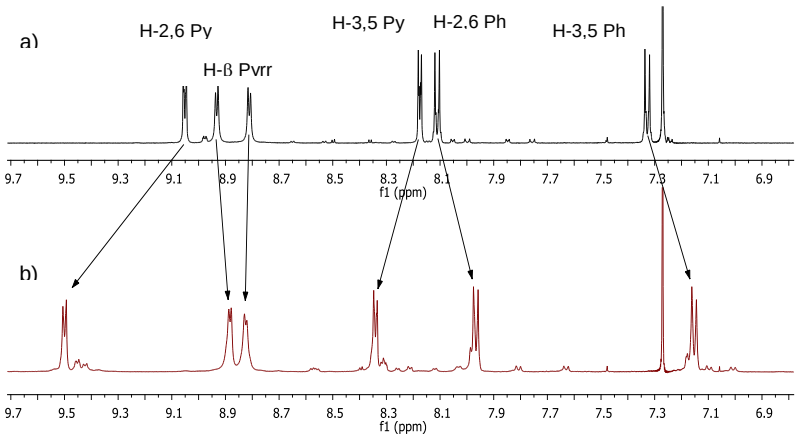

Figure 2. Downfield region of the ^{1}H-NMR spectra (500 MHz, $CDCl_3$) of a) DiTegPhDPyP, b) $[Re(CO)_3(DiTegPhDPyP)Br]_4$. For proton labelling see Scheme 1. For the full spectra see Supplementary Material.

Figure 2 shows the downfield region of the ^{1}H-NMR spectrum (500 MHz, $CDCl_3$) of $[Re(CO)_3(DiTegPhDPyP)Br]_4$ in comparison with that of the parent porphyrin DiTegPhDPyP. The number and the pattern of the signal of the porphyrin is maintained in the metallacycle, suggesting the formation of a highly symmetric cyclic structure. Moreover, the chemical shifts are in good agreement with those reported for other related metallacycles. The absence of signals corresponding to the protons of the free pyridine indicates that all the available pyridine fragments are bound to the Re(I) center, as also confirmed by the downfield shift of the H-2,6 of the pyridyl moieties as compared to the porphyrin precursor ($\Delta\delta$ = + 0.50 ppm). A smaller downfield shift ($\Delta\delta$ = + 0.26 ppm) is also observed for the neighboring H-3,5 protons, less influenced by coordination to the metal ion. The remaining signals are instead slightly upfield shifted, probably as a consequence of the shielding effect caused by the facing porphyrin aromatic walls within the metallacycle. The spectrum shows also some less intense resonances, for example to the right of the H-2,6 pyridyl

signals, which may be due to the presence of conformers, or to small amounts of impurities. VT-NMR experiments, performed from 0 up to + 50 °C, show the expected sharpening of all the peaks on increasing the temperature, with no simplification of the signals pattern, suggesting that, if the minor resonances are due to the presence of small amounts of conformers, these are not interconverting, at least in the temperature range explored (see Supplementary Material and below).

In the ^{13}C-NMR spectrum of $[Re(CO)_3(DiTegPhDPyP)Br]_4$ (Figure 3) the presence of only two signals (δ = 195.5, 192.7 ppm), in approximate 2:1 ratio, corresponding to the three carbonyl groups of the metal centre is in full agreement with the formation of the symmetric metallacycle, with a preserved *facial* disposition of these groups. Also in this case, a downfield shift of the C-2,6 and C-3,5 pyridyl signals ($\Delta\delta$ = + 4.8 and 2.3 ppm, respectively) can be observed. Regrettably, the solubility of the metallacycle is still too low to allow a full assignment of the ^{13}C-NMR spectra with HSQC experiments.

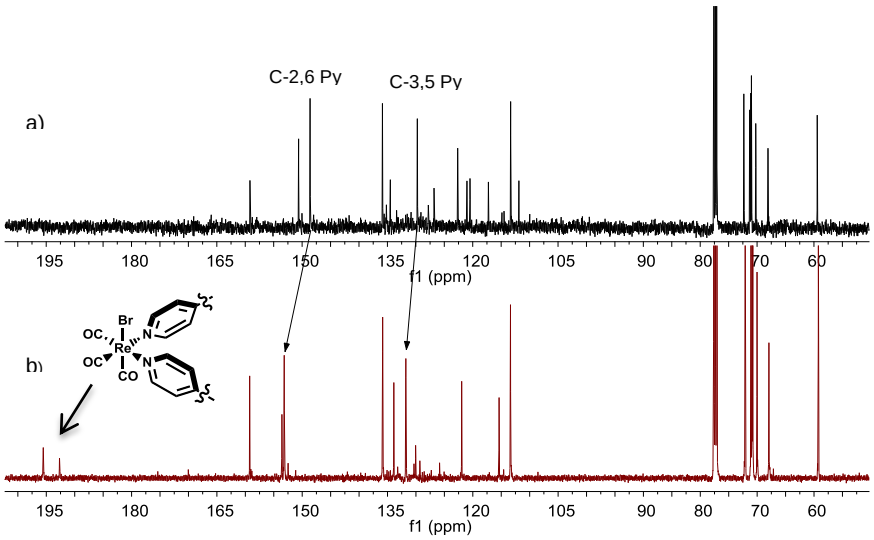

Figure 3. ^{13}C-NMR spectra (125 MHz, $CDCl_3$) of a) DiTegPhDPyP, b) $[Re(CO)_3(DiTegPhDPyP)Br]_4$.

Pulsed-field-gradient NMR experiments (Dbppste_cc Varian sequence) performed on both the porphyrin and the metallacycle, under the same experimental conditions (solvent, temperature and diffusion delay time), revealed that the two species diffuse with a net different rate, as it can be observed from the superimposed 2D maps of the ^{1}H DOSY spectra in Figure 4 (for the individual species ^{1}H DOSY spectra see the Supplementary Material).

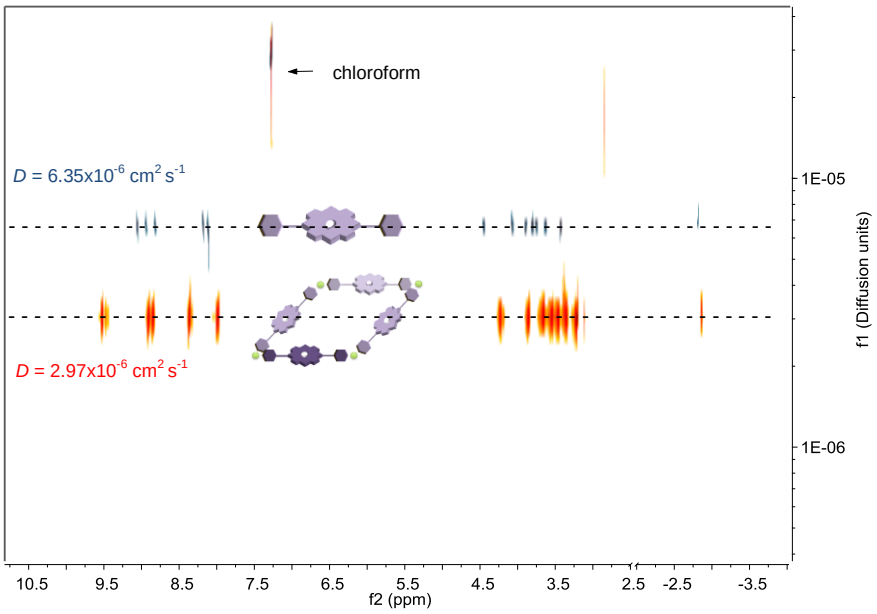

Figure 4. Superimposition of the ^{1}H DOSY-NMR 2D maps (500 MHz, $CDCl_3$, 298K, 100 ms diffusion delay) of DiTegPhDPyP (in blue) and of $[Re(CO)_3(DiTegPhDPyP)Br]_4$ (in red). The diffusion coefficients calculated for the two species are also indicated in the figure.

A qualitative inspection of Figure 4 clearly indicates that each of the two species diffuse as single molecules because all the corresponding resonances are aligned on the same diffusion coefficient value. Quantitative analysis of the ^{1}H signals decays allow for the determination of the diffusion coefficients, calculated according to equation 1 [23]:

$$ln(I_g/I_0) = -(\gamma^2\delta^2G^2(\Delta - \delta/3))D \quad (1)$$

where I_g and I_0 are the resonating peak intensity at the end and at the beginning of the pulse sequence, respectively, γ is the gyromagnetic ratio, G is the pulsed field gradient strength, Δ is the time separation between the pulsed-gradients, δ is the duration of the pulse and D is the diffusion coefficient. The product $\gamma^2G^2\delta^2(\Delta-\delta/3)$ is named as b value. Thus, a plot of $\ln(I_g/I_0)$ versus b for an isotropic solution should give a straight line, the slope of which is equal to $-D$ (see Figures S11 and S12). The diffusion coefficient obtained for the porphyrin (D = 6.35×10^{-6} ± 1.03×10^{-8} cm^{2}s^{-1}) is more than the double of that obtained for the metallacycle (D = 2.97×10^{-6} ± 1.09×10^{-8} cm^{2}s^{-1}), indicating that the porphyrin diffuses in solution at a rate that is about twice of the one measured for the metallacycle.

Applying the Stokes-Einstein equation (eq. 2), where R_h is the hydrodynamic radius, k_B is the Boltzmann's constant, T the absolute temperature, η is the dynamic viscosity of the solvent and

D is the diffusion coefficient, under the assumption that the molecules can be considered inscribed in a sphere [11], hydrodynamic diameters of 1.3 nm and 2.7 nm can be estimated, for the porphyrin and for the metallacycle, respectively. Although, in the absence of a calibration curve, these numbers cannot be taken as absolute values, they give a good and reliable indication of the relative size of the two systems, that is consistent with the formation of a metallacycle, rather than polymeric or concatenated products. Moreover, the D values correspond to the correct size range of the porphyrin (1.5 nm) and of the metallacycle (3.2 nm), as estimated from the X-ray structure and from an Avogadro molecular model, respectively.

$$R_h = k_B T / 6\pi\eta D \qquad (2)$$

With the aim to validate the data presented above, we also performed VT ^{1}H DOSY-NMR experiments on the metallacycle. In fact, by increasing the temperature the diffusion coefficient should increase, because the solvent viscosity decreases, while the R_h should remain constant, within the experimental errors. Figure 5 shows the normalized $\ln(I_g/I_0)$ intensities *vs b* values for the different temperatures explored, together with the linear fit of the data. In each case a good linear fit of the data is obtained and, as expected, the slope of the lines increases with the temperature. The values of the diffusion coefficients obtained and of the calculated molecular diameters are reported in Table 1.

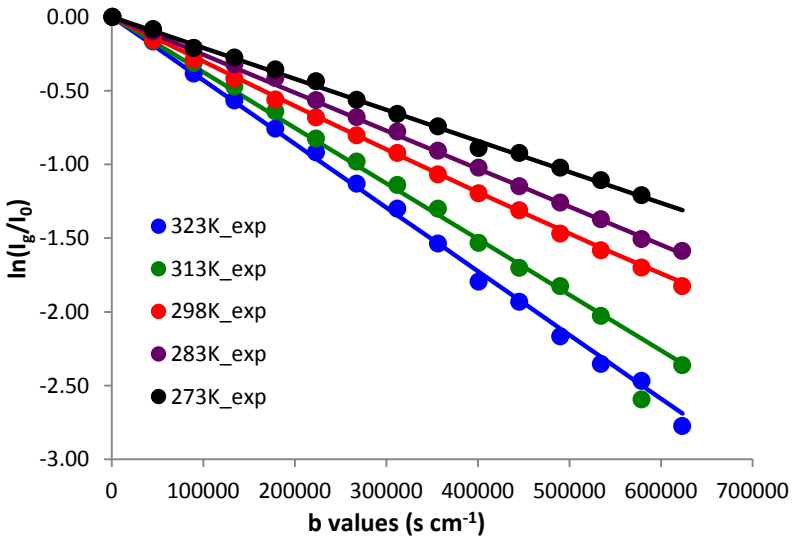

Figure 5. Plot of normalized $\ln(I/I_0)$ *vs b* for the more intense peak (MeO) of $[Re(CO)_3(DiTegPhDPyP)Br]_4$ at different temperatures (500 MHz, $CDCl_3$, 100 ms diffusion delay, temperature as indicated in the figure). The straight lines are the linear fit through the experimental data.

Table 1. Measured diffusion coefficients (*D*), solvent dynamic viscosity (η), and calculated diameters for $[Re(CO)_3(DiTegPhDPyP)Br]_4$ at different temperatures in $CDCl_3$. Dynamic viscosity data have been calculated by the Vogel equation using the Dortmund Data Bank (DDBST GmbH).

T (K)	*D* (cm^2s^{-1})	η (mPa·s)	Diameter (nm)
273	$2.09 \pm 0.03\times10^{-6}$	0.696	2.74
283	$2.56 \pm 0.04\times10^{-6}$	0.631	2.59
298	$2.97 \pm 0.01 \times10^{-6}$	0.542	2.71
313	$3.75 \pm 0.06 \times10^{-6}$	0.473	2.63
323	$4.30 \pm 0.06 \times10^{-6}$	0.434	2.56

The data reported in Table 1 show the increase of the metallacycle diffusion coefficient with the temperature while its diameter calculated with the Stokes-Einstein equation remain constant, with an average value of 2.65 ± 0.07 nm.

Interestingly, ^{1}H DOSY-NMR experiments may give important information about the homogeneity and purity of a sample. As said above the ^{1}H-NMR of $[Re(CO)_3(DiTegPhDPyP)Br]_4$ (Figure 2) shows some less intense extra peaks which may be due to the presence of impurities or to different conformations of the metallacycle. Figure 6 reports the intensity signals decays (lnI_g) versus *b* for the methoxy peak resonance (the most intense, belonging to the main species) and for an extra resonance near the H-2,6 pyridyl peak at 298 K (See also Figure S13 for the VT ^{1}H DOSY-NMR). The diffusion coefficients, obtained from the slope of the two lines, are identical suggesting that the two resonances belong to protons of the same compound or, at least, of two compounds with very similar sizes. Therefore, it appears that the extra resonances are more likely due to lower-symmetry conformers, rather than sample contamination by impurities.

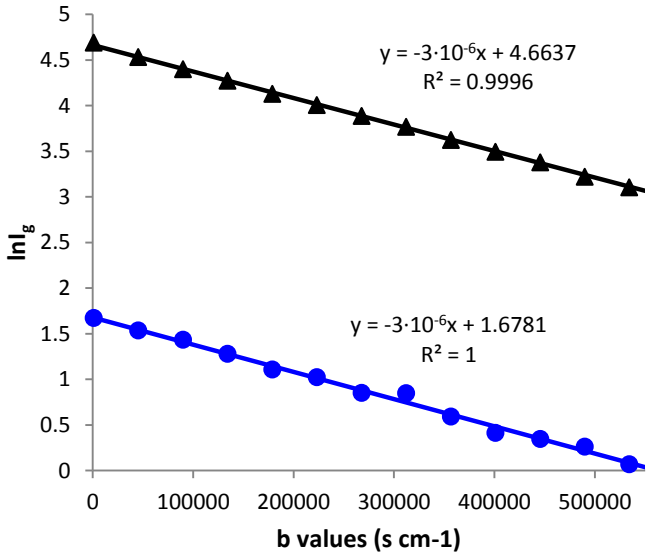

Figure 6. Plot of $\ln I_g$ *vs b* for the methoxy peak resonance (the most intense, belonging to the main species, black triangles) and for an extra resonance near the H-2,6 pyridyl peak major resonance (blue circles) (298K, $CDCl_3$, 100 ms). The lines are the linear fit of the experiment points.

3.2.2 Spectroscopic characterization of the $[Re(CO)_3(DiTegPhDPyP)Br]_4$ metallacycle

The metallacycle was further characterized by IR, UV-Vis and emission spectroscopy. The FT-IR spectrum of $[Re(CO)_3(DiTegPhDPyP)Br]_4$, in comparison with that of the parent porphyrin, shows the characteristic three strong bands (ν = 2024, 1921 and 1887 cm^{-1}) distinctive of three CO groups bound to Re(I) in a *facial* geometry (Figure 7).

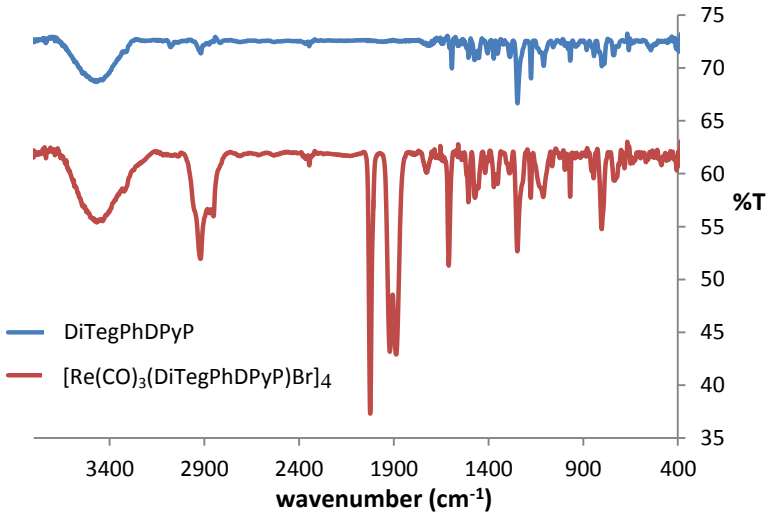

Figure 7. IR spectra in KI of DiTegPhDPyP (blue, top) and $[Re(CO)_3(DiTegPhDPyP)Br]_4$ (red, bottom).

The UV-Vis spectrum of the metallacycle in DCM (Figure 8) displays a 7.0 nm bathochromic shift of the Soret band respect to that of the porphyrin (λ_{max} DiTegPhDPyP = 419 nm; λ_{max} $[Re(CO)_3(DiTegPhDPyP)Br]_4$ = 426 nm), indicative of a net removal of electron density from the porphyrin macrocycle upon coordination of the pyridyl nitrogen to the rhenium center. Finally, the observed reduced emission intensity of the metallacycle, with respect to the parent porphyrin (Figure 9) can be ascribed to the heavy atom quenching effect exerted by the rhenium metal.

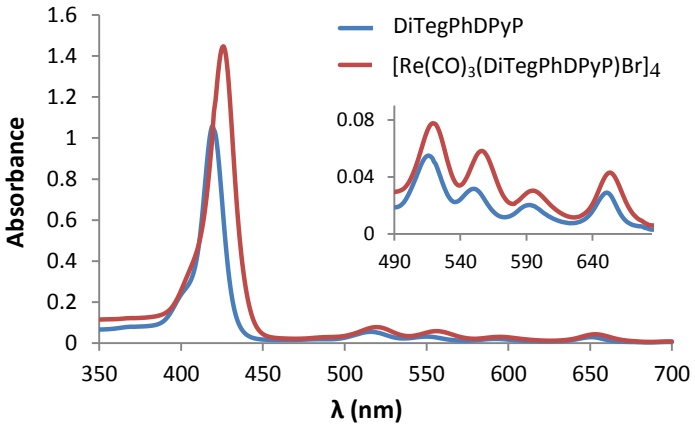

Figure 8. UV-Vis spectra of DiTegPhDPyP (blue) and $[Re(CO)_3(DiTegPhDPyP)Br]_4$ (red) in CH_2Cl_2 at *ca.* 2×10^{-6} M concentration (calculated with respect to the porphyrin units). The inset shows an enlargement of the Q bands region.

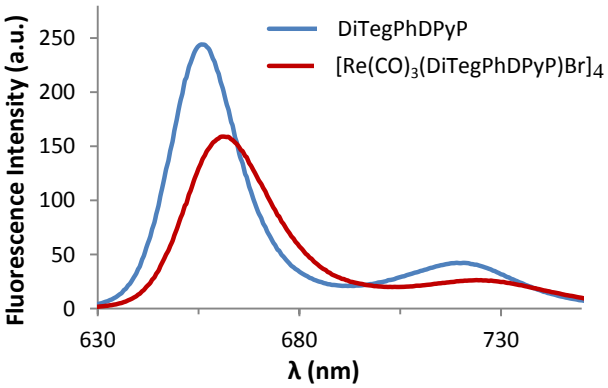

Figure 9. Fluorescence emission spectra of DiTegPhDPyP (blue) and $[Re(CO)_3(DiTegPhDPyP)Br]_4$ (red) in CH_2Cl_2 at *ca.* 2×10^{-6} M concentration (calculated with respect to the porphyrin units), λ_{exc} = 426 nm.

3.2.3 Atomic Force Microscopy

Next, the nano-aggregation of $[Re(CO)_3(DiTegPhDPyP)Br]_4$ on a solid substrate was investigated with Tapping-Mode Atomic Force Miscroscopy (TM-AFM). Indeed, there is interest in the formation of nano-aggregates and, in particular, in the formation of circular porphyrin arrays owing to their resemblance to the light-harvesting complexes of natural photosynthetic antennas [24]. Beautiful STM images of covalently linked porphyrin rings both in monomeric and aggregate form have been reported by H. L. Anderson and co-workers [25]. We also observed the formation of the so-called porphyrin 'rings' or 'nanocraters' by spraying a dioxane solution of the metallacycle ($c = 10^{-5}$ M) on a heated mica substrate (473 K). Analysis of Figure 10 shows the formation of regular, well defined ring like structures, well distributed on the mica surface, with an apparent diameter of about 0.1 μm. The three-dimensional view of a single aggregate (Figure 10c) shows that the ring core is empty and the walls are high about 1.2 nm suggesting that they are constituted by a single layer of porphyrin metallacycles. The formation of such nano-aggregates is a complex phenomenon which has been attributed as an interplay between solvent evaporation with formation of sub-micrometer droplets and material accumulation at the droplet edges by substrate flow inside the droplets [26]. As a consequence, the formation of the aggregates is strongly influenced by the rate of solvent evaporation and by the nature of the organic substrate. This is observed also in our case and the drop-casting of a solution of $[Re(CO)_3(DiTegPhDPyP)Br]_4$ on mica at lower temperature (289 K) led to the formation of extended aggregates (Figure S15) while spraying a DiTegPhDPyP solution on a heated mica substrate yielded small globular aggregates (Figure S16).

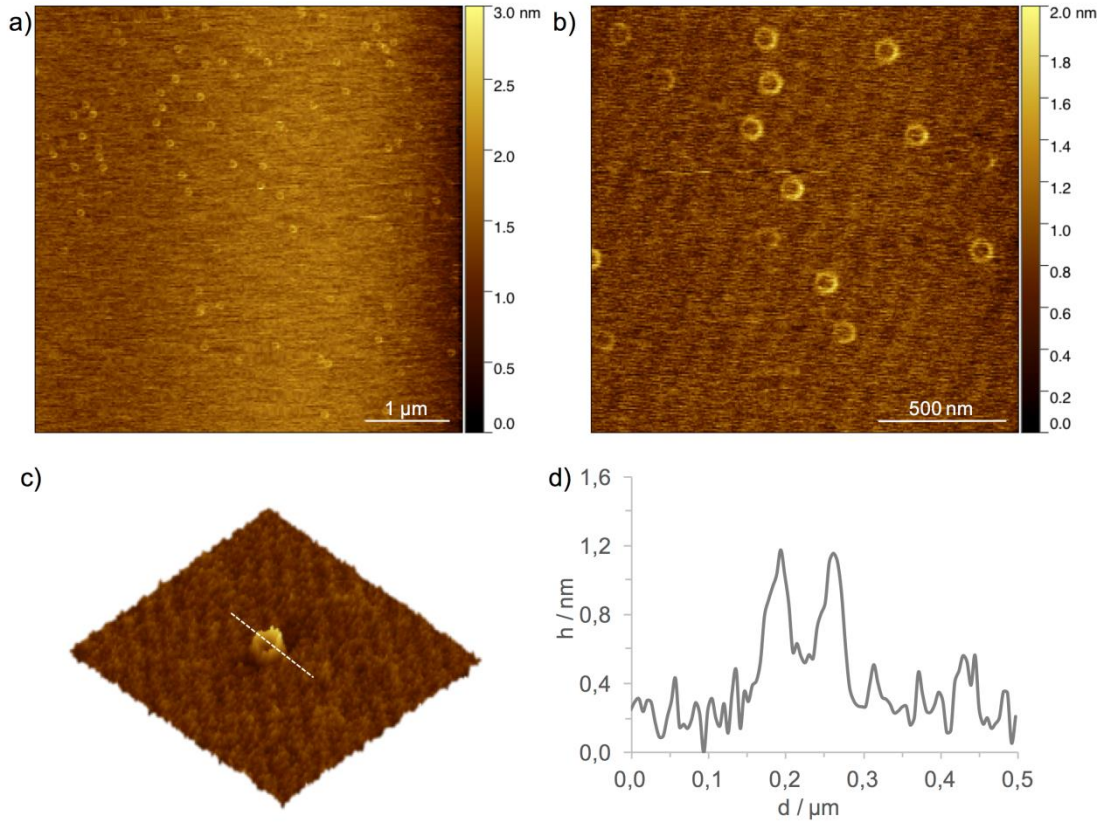

Figure 10. TM-AFM images of $[Re(CO)_3(DiTegPhDPyP)Br]_4$ sprayed on a heated mica substrate (473 K). a, b) Typical images of observed rings; c) three-dimensional view of a single ring and d) its height profile along the dashed line.

4. Conclusions

In conclusion we have reported the optimized synthesis and the full characterization, including the X-ray structure determination, of a polar *trans*-dipyridylporphyrin functionalized with two short polyoxyethylene chains. Following the metal-mediated directional-bonding approach, the porphyrin was then used to form a 4+4 metallacycle with Re(I) corners. In respect to analogous porphyrin cyclic derivatives, this adduct proved to be more soluble in common organic solvents and displayed a lower tendency to aggregate, thus allowing a full NMR characterization including VT ^{1}H DOSY-NMR experiments and, for the first time, the recording of a ^{13}C-NMR spectrum. Moreover, preliminary experiments of deposition of the metallacycle on an heated mica substrate show a tendency to self-organization with formation of regular ring-like nano-structures which are not formed by the parent porphyrin. The availability of these novel and more accurate NMR data gives further insight into the structural definition of these type of metallacycles, still remaining partly elusive for the incapability to obtain suitable single crystals for X-ray analysis, and

meaningful mass-spectroscopy data. Work is in progress in this direction and in the further characterization of the observed self-organization behavior on solid surfaces.

Acknowledgments

We thanks Prof. Davide Bonifazi (University of Cardiff) for helpful discussion. This work was supported by Fondazione Beneficentia Stiftung, and UNITS-FRA_2014 and _2015 projects.

Supplementary Material

^{1}H-NMR and ^{13}C-NMR spectra of DiTegPhDPyP and $[Re(CO)_3(DiTegPhDPyP)Br]_4$, CCDC 1475279 contains the supplementary crystallographic data for this paper. These data can be obtained free of charge from The Cambridge Crystallographic Data Centre via www.ccdc.cam.ac.uk/data_request/cif.

References

[1] a) T. R. Cook, P. J. Stang, Chem. Rev. 115 (2015) 7001; b) N. J. Young, B. P. Hay, Chem. Commun. 49 (2013) 1354; c) M. M. J. Smulders, I. A. Riddell, C. Browne, J. R. Nitschke, Chem. Soc. Rev. 42 (2013) 1728.

[2] S. Leininger, B. Olenyuk, P. J. Stang, Chem. Rev. 100 (2000) 853.

[3] a) F. Scandola, C. Chiorboli, A. Prodi, E. Iengo, E. Alessio, Coord. Chem. Rev. 250 (2006) 1471; b) I. Beletskaya, V.S. Tyurin, A.Y. Tsivadze, R. Guilard, C. Stern, Chem. Rev. 109 (2009) 1659.

[4] E. Iengo, P. Cavigli, D. Milano, P. Tecilla, Inorg. Chim. Acta 417 (2014) 59.

[5] S.J. Lee and J.T. Hupp, Coord. Chem. Rev. 250 (2006) 1710.

[6] a) M. Boccalon, E. Iengo, P. Tecilla, J. Am. Chem. Soc. 134 (2012) 20310; b) F. De Riccardis, I. Izzo, D. Montesarchio, P. Tecilla, Acc. Chem. Res. 46 (2013), 2781.

[7] U. Devi, J. R. D. Brown, A. Almond, S. J. Webb, Langmuir 27 (2011) 1448.

[8] R. V. Slone, J. T. Hupp, Inorg. Chem. 36 (1997) 5422.

[9] M. H. Keefe, J. L. O'Donnell, R. C. Bailey, S. T. Nguyen, J. T. Hupp, Adv. Mater. 15 (2003) 1936.

[10] C. R. Graves, M. L. Merlau, G. A. Morris, S.-S. Sun, S. T. Nguyen, J. T. Hupp, Inorg. Chem. 43 (2004) 2013.

[11] W. H. Otto, M. H. Keefe, K. E. Splan, J. T. Hupp, C. K. Larive, Inorg. Chem. 41 (2002) 6172.

[12] L. Miljacic, L. Sarkisov, D. E. Ellis, R. Q. Snurr, J. Chem. Phys. 121 (2004) 7228.

[13] M. Boccalon, E. Iengo, P. Tecilla, Org. Biomol. Chem. 11 (2013) 4056.

[14] C. Ruziè, L. Michaudet, B. Boitrel, Tetrahedron Lett. 43 (2002) 7423.

[15] S. Pisano, D. Milano, N. Passoni, E. Iengo, P. Tecilla, J. Porphyrins Phthalocyanines 20 (2016) 514.

[16] S. P. Schmidt, W. C. Trogler, F. Basolo, Inorg. Synth. 28 (1990) 160.

[17] W. Kabsch, Acta Cryst. D66 (2010) 125.

[18] M. C. Burla, R. Caliandro, B. Carrozzini, G. L. Cascarano, C. Cuocci, C. Giacovazzo, M. Mallamo, A. Mazzone, G. Polidori, J. Appl. Cryst. 48 (2015) 306.

[19] G. M. Sheldrick, Acta Cryst. A64 (2008) 112.

[20] M. Ravikanth, J-P. Strachan, F. Li, J. S. Lindsey, Tetrahedron 54 (1998) 7721.

[21] R. Chakrabarty, P. S. Mukherjee, P. J. Stang, Chem. Rev. 111 (2011) 6810.

[22] J. T. Hupp, Struct. Bond. 121 (2006) 145.

[23] Y. Cohen, L. Avram, L. Frish, Angew. Chem. Int. Ed. 44 (2005) 520.

[24] a) A. P. H. J. Schenning, F. B. G. Benneker, H. P. M. Geurts, X. Y. Liu, R. J. M. Nolte, J. Am. Chem. Soc. 118 (1996) 8549; b) C. R. L. P. N. Jeukens, M. C. Lensen, F. J. P. Wijnen, , J. A. A. W. Elemans, P. C. M. Christianen, A. E. Rowan, J. W. Gerritsen, R. J. M. Nolte, J. C. Maan, Nano Lett. 4 (2004) 1401.

[25] a) M. C. O'Sullivan, J. K. Sprafke, D. V. Kondratuk, C. Rinfray, T. D. W. Claridge, A. Saywell, M. O. Blunt, J. N. O'Shea, P. H. Beton, M. Malfois, H. L. Anderson, Nature 469 (2011) 72; b) S. A. Svatek, L. M. A. Perdigão, A. Stannard, M. B. Wieland, D. V. Kondratuk, H. L. Anderson, J. N. O'Shea, P. H. Beton, Nano Lett. 13 (2013) 3391.

[26] a) L. Latterini, R. Blossey, J. Hofkens, P. Vanoppen, F. C. De Schryver, A. E. Rowan, R. J. M. Nolte, Langmuir 15 (1999) 3582; b) T. Marangoni, S. A. Mezzasalma, A. Llanes-Pallas, K. Yoosaf, N. Armaroli, D. Bonifazi, Langmuir 27 (2011) 1513.